Tech Science Press

Determination of a Safe Distance for Atomic Hydrogen Depositions in Hot-Wire Chemical Vapour Deposition by Means of CFD Heat Transfer Simulations

Lionel Fabian Fourie[1] and Lynndle Square[2,*]

[1]Department of Physics and Astronomy, University of the Western Cape, Bellville, 7535, South Africa
[2]Department of Physics, North-West University, Potchefstroom, 2520, South Africa
*Corresponding Author: Lynndle Square. Email: lynndle.square@nwu.ac.za

Abstract: A heat transfer study was conducted, in the framework of Computational Fluid Dynamics (CFD), on a Hot-Wire Chemical Vapour Deposition (HWCVD) reactor chamber to determine a safe deposition distance for atomic hydrogen produced by HWCVD. The objective of this study was to show the feasibility of using heat transfer simulations in determining a safe deposition distance for deposition of this kind. All CFD simulations were set-up and solved within the framework of the CFD packages of OpenFOAM namely; snappyHexMesh for mesh generation, buoyantSimpleFoam and rhoSimpleFoam as the solvers and paraView as the post-processing tool. Using a standard set of deposition parameters for the production of atomic hydrogen by HWCVD, plots of the gas temperature in the deposition region were produced. From these plots, we were able to determine a safe deposition distance in the HWCVD reactor to be in the range between 3 and 4 cm from the filament.

1 Introduction

Hot-wire Chemical Vapour Deposition (HWCVD), is an elegant low pressure deposition technique used for the deposition of functional thin films. Since its first patent in the early 1980s [1–3], the HWCVD technique has been improved considerably and is currently a viable method for the deposition of many different functional films, both organic and inorganic.

The HWCVD technique is based on the decomposition of precursor gasses at a catalytic hot surface. The resulting radicals formed from this decomposition interact with the molecules at the surface of the substrate forming the desired film. In principle, the technique is simple and reliable. However, slight changes in any of the deposition parameters can lead to a large number of undesired defects appearing in the material severely compromising the quality of the films. Since repeatability is a key aspect of any experiment, adequate time should be taken to understand the layout and geometry of the HWCVD reaction chamber as well as how different deposition parameters will affect the quality of the resulting film. Unfortunately, conducting multiple trial experiments to achieve this end becomes expensive and time consuming. This is where Computational Fluid Dynamics (CFD) and material modeling becomes an invaluable tool. By developing a functional computer model of the system, the experimentalist obtains the ability to run multiple

simulations, using different deposition parameters, to ascertain which would suit their film growth requirements best before conducting any experiment.

The main deposition parameters to consider in the HWCVD technique are: catalytic surface or filament temperature (T_f), substrate temperature (T_{sub}), number of filaments, or loops if a coil is used, distance between the filaments and substrate (d_{f-s}), the overall temperature of the reaction chamber (T) and the gas flow rate. The control of these parameters is key to understanding the HWCVD process as well as ensuring high quality films are grown during every deposition.

In this work, the authors, through CFD simulations, focus on the temperature development inside the system's reaction chamber during a standard deposition process for the production of atomic hydrogen (H), from the catalytic decomposition of molecular hydrogen (H_2). The main goal of this study was to determine a safe deposition distance (d_{f-s}) for the CADAR HWCVD reactor. Sali et al. [4] conducted a growth simulation study using a one-dimensional numerical model, in a HWCVD reactor, for the film thickness uniformity using a SiH_4 precursor gas.

In their work, they deduced that the d_{f-s} distance is proportional to the number of filaments used during the deposition as well as the inter-filament separation. Their model showed that a d_{f-s} distance for 4 filaments, with inter-filament separation of 15 mm, was 25 mm at a chamber pressure of 1.3 Pascal (Pa). Lee et al. [5] conducted a similar study on the influence of filament temperature on the crystallographic properties of poly-silicon films prepared by HWCVD process. In it, they used Surface Electron Microscopy (SEM) images to deduce a d_{f-s} distance of 20 mm, with T_f of 1800°C, and 40 mm, with T_f of 2000°C, that would ensure a T_{sub} of 400°C. In work done by Schüttauf et al. [6] on the pre-deposition passivation of crystalline silicon by a-Si: H with atomic hydrogen using HWCVD, they outlined the factors to consider when determining the safe d_{f-s} distance. These factors include; the atomic H-flux, the etching rate of atomic H on the substrates and the substrate temperature that would promote atomic H bonding with the substrates while also minimizing the etching rate. In their work, Schüttauf et al. used a filament temperature of 1980°C at a d_{f-s} distance of 20 cm with a significantly high substrate temperature (> 100°C). These parameters were chosen to suppress surface etching on the c-Si wafers. The atomic H-flux is directly proportional to the temperature of the filament which means that an increase in filament temperature would increase the rate of production of atomic H as outlined in a study by Umemoto et al. [7] in which a combination of a two-photon laser-induced fluorescence (LIF) technique and a vacuum ultraviolet (Lyman α) absorption technique is used to determine the absolute H-atom densities. Umemoto et al. also reported an atomic H density of 1.5×10^{14} cm^{-3} at 10 cm from the filament with a temperature of 1927°C. From this result, they concluded that the filament temperature should be varied, depending on the type of substrate used in the deposition, to limit the damage to the substrate caused by the H atoms. Given that the HWCVD reactor used in our study has a maximum d_{f-s} distance of 10 cm, it is important to know the gas temperature in this region as this can be used determine the optimal distance from the filament to place the substrates during the deposition. The temperature of the gas at different points can provide a reasonable approximation for the energy of the gas which can then be used to limit the etching rate on the substrates. Hence, in this work, we try to demonstrate the feasibility of using heat transfer simulations in determining a safe d_{f-s} distance as opposed to using experimental methods to do so. In doing so, experimentalists would obtain a quick and efficient way of determining a safe d_{f-s} distance without the need to conduct multiple trial and error experiments to achieve this.

2 Computational Procedure

The approach taken to study the heat transfer inside the HWCVD reaction chamber was to decompose the study into two separate cases, hereafter referred to as Case 1A and Case 1B. In the model, the different components of the HWCVD chamber are assigned an emissivity value that corresponds to the emissivity value of the material it is fabricated from. The filament is modeled as a heat source, made from 99.9%

tungsten, with an emissivity of 0.35. This was done to ensure that the different components of the model respond to the increase in heat as accurately as possible. In Case 1A, the intent was to map the temperature radiation from the filaments as well as map the radiation intensity from the different components of the system before the precursor gas is introduced into the system. There is no flow emanating from the inlet in this case so that the temperature distribution under radiative transport can be studied effectively. For Case 1B, the goal was to study and map the temperature changes that occur after the introduction of the precursor gas into the system while also determining a safe deposition distance between the filaments and the substrate. All simulations of the system are run using two heat transfer solvers from the open-source CFD software OpenFOAM, namely, buoyantSimpleFoam (Case 1A) and rhoSimpleFoam (Case 1B). buoyantSimpleFoam is listed as a steady-state solver for buoyant and turbulent flow of compressible fluids [8], whereas rhoSimpleFoam is listed as a steady-state solver for laminar or turbulent Reynolds Average Navier Stokes (RANS) flow of compressible fluids [9]. OpenFOAM primarily uses the Finite Volume Method (FVM) in solving CFD cases [10].

2.1 Mesh Generation

A computational geometry, that replicated the CADAR system, was created from measurements taken of the CADAR deposition system at the University of the Western Cape Department of Physics and Astronomy. The replicated geometry was subsequently then used to generate the computational domain or mesh. The CADAR is a multi-chamber ultra-high vacuum deposition system used for the growth and refinement of high quality films. The system comprises two separate Plasma-Enhanced CVD reactor chambers, two HWCVD reactor chambers, a thermal evaporation chamber and a transfer chamber all separated by valves that allow each chamber to be kept at different pressures. For this study, the authors focus solely on the HWCVD chamber of the system that is connected to one Plasma reaction chamber. No valves are separating the two reaction chambers so they are considered to be a single chamber with two separate sources for deposition.

The system in Fig. 1 is reproduced using the Computer Aided Design (CAD) software FreeCAD, based on the physical measurements taken of the system's internal and external geometry. The front- and top-view of the CAD model is illustrated in Fig. 2. The 3D mesh is then created from the CAD model using one of the built-in pre-processing tools of OpenFOAM called snappyHexMesh to ensure mostly hexahedral cells are used which subsequently simplifies the simulation process. During the process of creating the mesh, boundary conditions are added to the different components of the system namely, the filaments and its holder, the substrate holder as well as the gas inlet and outlet. The final mesh is illustrated in Fig. 3 with a summary of the mesh statistics given in Tab. 1.

Figure 1: HWCVD reactor chamber of the CADAR system

2.2 Mesh Independency Study

To establish the accuracy of the CFD solution, and minimize the computational costs, the precursor gas temperature was analyzed using: the rhoSimpleFoam solver along with the standard k-ε model with the wire at uniform T = 1873 K (1600°C) with mass flow rate of $8.98e^{-8}$ kg/s (60 sccm) for the H_2 precursor gas. The
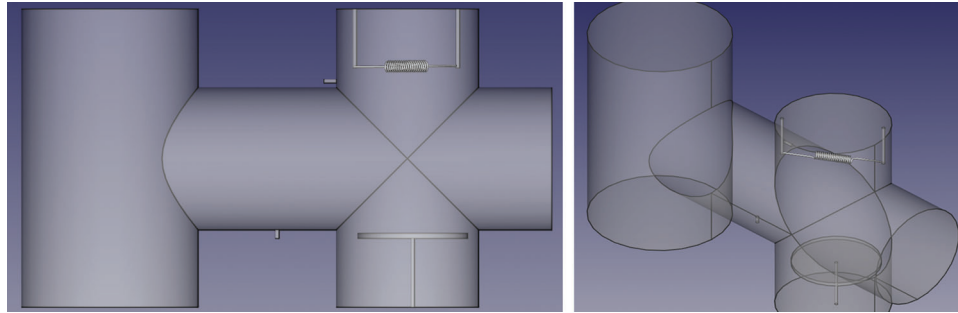
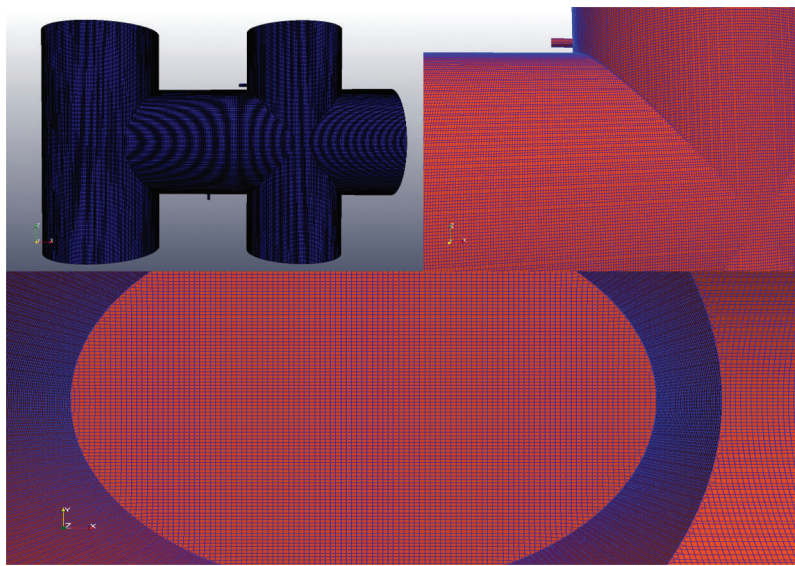**Figure 2:** Front-view (left) and top-view (right) of the CAD model of the HWCVD reactor

Figure 3: Surface mesh generated from the CAD model

Table 1: Mesh statistics

Cell Shape	Number of cells of each type
Hexahedra	16555936
Prisms	141395
Pyramids	0
Tet Wedges	3
Tetrahedra	1
Polyhedra	1866

grid convergence study was conducted by developing three different meshes: with a coarse, medium and fine grid to predict the gas temperature at a fixed distance, 10 mm, away from the wire to determine how the mesh quality affects the CFD simulation results. The number of nodes and the simulation runtime for the three cases is highlighted in Tab. 2.

Table 2: Mesh size, CFD runtime and estimated temperature after 300 iterations

Mesh Resolution	Coarse Mesh	Medium Mesh	Fine Mesh
Number of Nodes	5056859	12863164	23146319
Simulation Runtime	1 hrs 7 mins	3 hrs 20 mins	6 hrs 10 mins
Estimated Temperature (°C)	527.96	296.74	296.39

In the mesh independence study, three mesh types, from coarse to fine, were generated to ensure that the simulation results were significantly grid-independent. As shown in Tab. 2, when the number of nodes is higher than 12863164, the temperature at the reference location, 10 mm away from the wire, becomes stable and remained nearly unchanged. Accounting for computational efficiency, the mesh with 12863164 nodes was used for further simulation.

2.3 Simulation Parameters and Algorithm Control

After the mesh was created, a copy was pasted into the file directory of each case where each case can be solved separately. In Case 1A, it was assumed that the only mode of heat transfer that can occur in the reactor was heat transfer by means of radiation. This was mainly due to there being no medium present inside the reactor i.e., no precursor gas is flowing into the reactor chamber, as well as low pressures, ~10^{-6} mbar, inside the reactor during the simulation. This results in heat transfer due to conduction and convection becoming negligible. A second order scheme, bounded using a Sweby limiter of 0.2, was used to discretize the transport equations for momentum, heat and mass. A numerical scheme called a Preconditioned Conjugate Gradient (PCG) algorithm is used as a solver for the pressure (p) and the pressure without the hydrostatic pressure (p_{rgh}). A convergence criterion of 1×10^{-3} was applied to the residuals of the continuity, momentum and energy equations for Case 1A.

In Case 1B, all three modes of heat transfer are assumed to be feasible because in this case a medium, the precursor gas H_2, is allowed to flow into the reactor chamber and interact with the catalytic filaments. The model uses Sutherland's Law to solve the transport equation which solves the dynamic viscosity as a function temperature. The selections for the fluid properties as well as the Sutherland coefficients of the precursor gas are listed in Tab. 3. A first order upwind scheme was used to discretize the transport equations for momentum, heat and mass. The numerical scheme called Geometric agglomerated Algebraic Multi-Grid (GAMG) is used to solve for p, velocity ($\mathbf{u}$) and internal energy (e). A convergence criterion of 1×10^{-3} was applied to the residuals of continuity and energy equations whilst a criterion of 1×10^{-4} was applied to the residuals of momentum to improve the result accuracy.

For both cases, The SIMPLE algorithm was used for the pressure-velocity coupling as our case is steady-state with a high Relaxation factor being defined for enthalpy (h), Case 1A, and e, Case 1B, to force the solution to converge. The convergence criteria for both cases, which were found using the trial and error approach, fit the simulations best as they offered a balance between execution time and the accuracy of the results.

Table 3: Fluid parameters for the precursor (H_2) gas

Fluid Parameter	Value	Unit
Density (H_2)	0.08988	g/L
c_p	14130	Pa s
Heat of Fusion	58.7	J/g
Sutherland Temperature (T_s)	96.67	K
Sutherland Coefficient (A_s)	6.89e-7	Kg/(m s (K)$^{1/2}$)

2.4 Model Equations

The following conservation equations for mass, momentum and thermal energy was used [11]:

Continuity equation:

$$\nabla \cdot (\rho \mathbf{u}) = 0 \tag{1}$$

where ρ is the density field and $\mathbf{u}$ is the velocity field.

Conservation of Momentum:

$$\nabla \cdot (\rho \mathbf{u} \mathbf{u}) = -\nabla p + \rho \mathbf{g} + \nabla \cdot \left(2\mu_{eff} \, D(\mathbf{u}) \right) - \nabla \left(\frac{2}{3} \mu_{eff} \left(\nabla \cdot \mathbf{u} \right) \right) \tag{2}$$

where p is the static pressure field and $\mathbf{g}$ is the acceleration due to gravity. The effective viscosity (μ_{eff}) is the sum of the molecular and turbulent viscosity, while $D(\mathbf{u})$ is the deformation tensor and is defined as $D(\mathbf{u}) = \frac{1}{2} \left(\nabla u + (\nabla u)^{T} \right)$.

In OpenFOAM, the pressure gradient and gravity force terms are implemented as follows:

$$-\nabla p + \rho \mathbf{g} = \nabla p_{rgh} - (\mathbf{g} \cdot \mathbf{r}) \nabla \rho \tag{3}$$

where $p_{rgh} = p - \rho \mathbf{g} \cdot \mathbf{r}$ and $\mathbf{r}$ is the position vector.

For the conservation of energy, each case is solved using a different energy solution variable. Case 1A uses enthalpy (h), Eq. (4), while Case 1B uses internal energy (e), Eq. (5). The conservation of energy equations take the following form:

$$\nabla \cdot (\rho \mathbf{u} h) + \nabla \cdot (\rho \mathbf{u} K) = \nabla \cdot \left(\alpha_{eff} \nabla h \right) + \rho \mathbf{u} \cdot \mathbf{g} \tag{4}$$

$$\nabla \cdot (\rho \mathbf{u} e) + \nabla \cdot (\rho \mathbf{u} K) + \nabla \cdot (p \mathbf{u}) = \nabla \cdot \left(\alpha_{eff} \nabla e \right) + \rho \mathbf{u} \cdot \mathbf{g} \tag{5}$$

where $K \equiv \frac{|\mathbf{u}|^2}{2}$ is the kinetic energy per unit mass; h is the sum of energy per unit mass, the internal energy and the kinetic energy i.e., $h \equiv e + \frac{p}{\rho}$. The effective thermal diffusivity, $e^{\frac{\alpha_{eff}}{\rho}}$, is the sum of the laminar and turbulent thermal diffusivities:

$$\alpha_{eff} = \frac{\rho v_t}{Pr_t} + \frac{\mu}{Pr} = \frac{\rho v_t}{Pr_t} + \frac{k}{c_p} \tag{6}$$

where k is the thermal conductivity, c_p is the specific heat at constant pressure, v_t is the turbulent viscosity, Pr is the Prandtl number and Pr_t is the turbulent Prandtl number.

Since both cases are solved using steady-state solvers, the time derivative is omitted from the conservation equations.

3 Results and Discussion

The set of deposition parameters used in this investigation is listed in Tab. 4 below. From this, two simulations were run to investigate the heat transfer inside the CADAR's HWCVD reactor chamber. The results of these simulations are presented below.

3.1 Case 1A

In this case, the objective was to study the effects of the coiled filament temperature, through radiation, on the temperature profile of the system before the precursor gas is introduced. The filament temperature is set to 1873 K as a baseline temperature for this study. Before the filaments are turned on, the internal

Table 4: Deposition parameters for the production of atomic H

Deposition Parameter	Value	Unit
Base pressure	6×10^{-6}	mbar
Deposition pressure	100	µbar
H_2 flow rate	60	sccm
Filament temperature	> 1873 (1600)	K (°C)

temperature is set 293 K (20°C). This simulation was set to run for 1000 iterations, along with the convergence criterion mentioned in Section 2.2, but converged after 783 iterations with an execution time of approximately 6.5 hours. The results of the simulation are verified graphically using the post-processing utility of OpenFOAM called paraView.

Fig. 4 illustrates the radiative temperature profile from the coiled filament which serves as the baseline measurements. A dissection of the reactor was performed, using the y-axis as the normal to the cutting plane, on the mesh to expose the internal components of the reactor. Key observations from this simulation are: how far from the filament the radiation emitted can still be felt, the temperature of the radiation 'cloud' surrounding the filament as well as the fact that the rest of the reactor vessel remains at the initial temperature of 293 K.
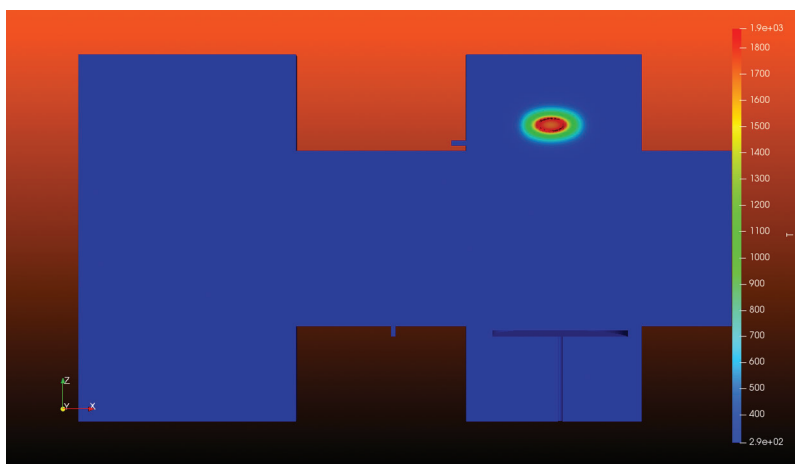
Figure 4: Radiative temperature profile of the HWCVD reactor (K)

3.2 Case 1B

In this case, the objectives were to model and study the heat transfer from the filaments to the precursor gas, map the temperature profile of the reactor as well as to determine a safe deposition distance, (d_{f-s}), between the filaments and the substrate. The d_{f-s} distance varies for every experiment and is dependent on how much of the radiation from the filaments the experimenter requires their substrate to absorb. As with Case 1A, the filaments were set to 1873 K and the internal temperature of the reactor set to 293 K. A volumetric flow rate at the inlet of the reactor was set to 60 standard cubic centimeters (sccm) for the precursor gas. This simulation was set to run for 1000 iterations, but convergence was achieved after 967 iterations with an execution time of around 8 hours.

The heat transfer temperature profile for the case with a gas flow into the reactor is illustrated in Fig. 5. When compared to Fig. 4, the simulation results in Fig. 5 show a substantial growth of the temperature
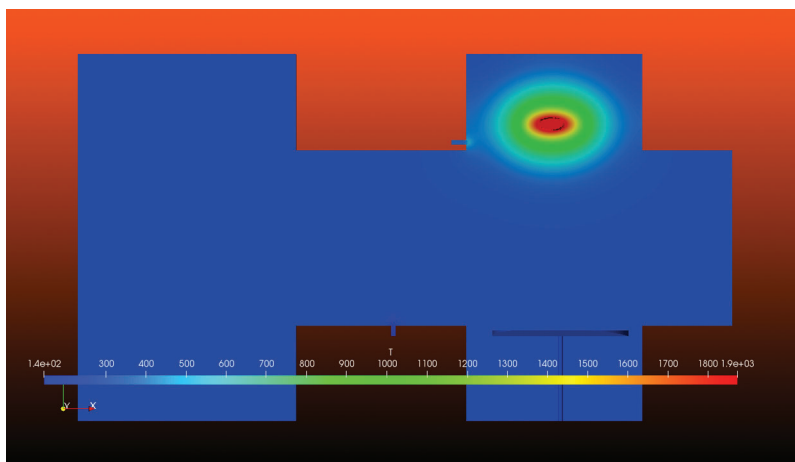
Figure 5: Heat transfer temperature profile of the HWCVD reactor (K)

'cloud' surrounding the coil. This increase is attributed to the absorption of energy, radiated by the coil, by the H_2 precursor gas as it approaches or makes contact with the coil. Upon its entry into the system, the precursor gas becomes a medium by which temperature is transported inside the system which subsequently increases the temperature in certain regions of the reactor during the deposition. To further compare the results from Figs. 4 and 5, the temperature as a function of distance is plotted for the area between the filament and the substrate holder, hereafter known as the deposition region. In Fig. 6, the results for Case 1A is presented as (Vacuum) with the results for Case 1B being presented as (with gas).
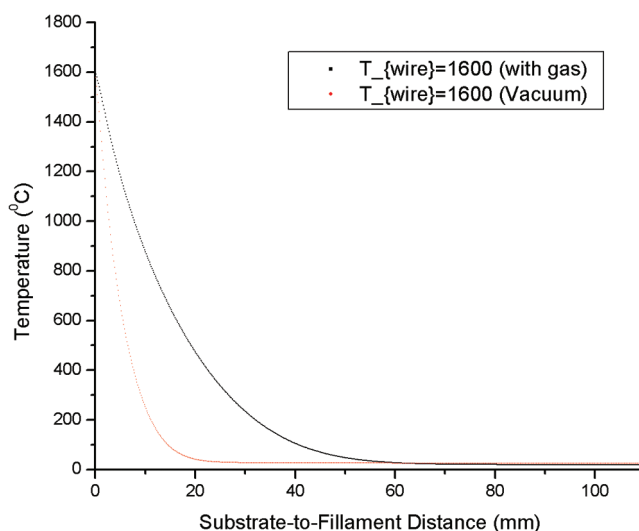

Figure 6: Substrate-to-Filament temperature plot for T_f = 1873 K (1600°C), 2073 K (1800°C) and 2273 K (2000°C)

In the substrate-to-filament distance plot, Fig. 6, zero mm corresponds to the surface of the coil with a temperature of 1600°C. As one moves away from the coil, the temperature drops drastically. This drop in temperature occurs much closer to the coil in for the vacuum case compared to the case with the H_2 gas flow into the reactor. Also evident in the substrate-to-filament distance plot is the large difference in temperature between the cases with and without gas flow. This difference stems from the addition of

conduction and convection to the modes heat transfer that comes with the flow of gas in the reactor. In other words, the temperature plot for the case with gas illustrates the gas temperature at various points from the filament. The temperature dissipation in the region appears to be proportional to $1/r^2$, where r is the distance from the coil. The significance of this is that temperature dissipates relatively quickly minimizing the heat transfer from the gas to the substrates. This, depending on the placement of the substrates, allows for better control over T_{sub} which ultimately suppresses morphological changes that can occur in the substrates due to excessive heating. Based on the plots in Fig. 6, we believe that a safe d_{f-s} distance in the CADAR HWCVD reactor to be in the range between 30 and 40 mm (3 and 4 cm) for the specific set of deposition parameters used. In this region, the gas temperature ranges from ~200°C to ~100°C which suggests that the gas still has enough energy to facilitate the transport of atomic H in the reactor [7]. The temperature in this region is also low enough to minimize heat transfer between the gas and the substrates as to not compromise the structural properties of the substrates. To verify these results, simulations were run with T_f = 2073 K (1800°C) and 2273 K (2000°C), with the H_2 gas flow into the reactor, whose temperature plots are then compared to the plots in Fig. 6. The result of this analysis is illustrated in Fig. 7.
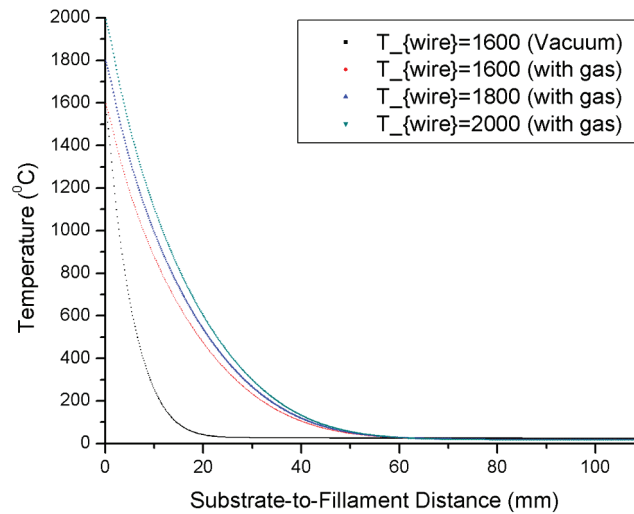

Figure 7: Substrate-to-Filament temperature plot for T_f = 1873 K (1600°C), 2073 K (1800°C) and 2273 K (2000°C)

Fig. 7 shows that the temperature dissipation in the model, for different filament temperatures, follows a similar trend inside the reactor. The temperature plots, for the three cases with gas, shows that the temperature in the deposition region stabilizes approximately 40 mm (4 cm) from the filament regardless of the filament temperature. At this point, the three plots converge at approximately 100°C after-which they tend towards room temperature, 20°C, at 60 mm and beyond. This result shows that even at higher filament temperatures, the gas temperature reaches a point of equilibrium in the proposed safe deposition region i.e., between 3 and 4 cm from the filament.

3.3 Model Validation

Due to the lack of comprehensive computational and experimental studies in which both the gas and substrate temperatures are recorded for the HWCVD process, the substrate surface temperature (T_{ss}), which is different to $T_{sub,}$ was used to validate the results of this study. According to, and in agreement with, Matsumura et al. [12] this is deemed to be an adequate approximation as only 30% of the total power supplied to the wire is dissipated by thermal radiation with the other 70% used for heat transport

of the heated precursor gas. In work done by Matsumura [13] on the formation of silicon based thin films prepared by HWCVD, he used a thermo-couple fixed to the surface of the substrate to measure the temperature at a fixed distance of 40 mm away from the wire which was set to a fixed temperature of 1700°C. In doing so, he recorded temperatures in the range between 200°C and 210°C for a fixed flow rate of 50 sccm of H_2 gas. In other work done by Karasawa et al. [14], with a similar setup to that used by Matsumura, recorded a T_{ss} in the range between 240°C and 320°C for a fixed d_{f-s} = 30 mm and T_f = 1900°C. Both sets of recorded data are in good agreement with the model data presented in Fig. 7 for the higher filament temperatures as for the two reported d_{f-s} distances, 30 and 40 mm, the temperatures are within the same range.

As demonstrated in the preceding model validation exercise, the numerical model used is in this study is capable of simulating temperature profiles in the HWCVD process and as such, the use of heat transfer simulations can thus be seen as a viable means of determining a safe d_{f-s} distance for atomic Hydrogen depositions in the HWCVD process.

4 Conclusion

In this work, the determination of a safe deposition distance for atomic hydrogen in a HWCVD reactor chamber was investigated. This was done through CFD heat transfer simulations using the CFD software OpenFoam. Using the temperature of the gas at different points in the deposition region, Figs. 6 and 7, we were able to deduce that a safe d_{f-s} distance for the reactor in question to be between 3 and 4 cm. In this region, temperatures are low enough to suppress any etching of the substrates while still being high enough to facilitate the transport of atomic H through the reactor vessel as outlined by Umemoto et al. [7]. The results also showed that using higher filament temperatures in the deposition has a minimal effect of the gas temperature in the deposition region as the temperature stabilizes after 4 cm from the filament. Since this is a macro-level study of the HWCVD reactor, we can only speculate about the value of the H density in the proposed safe deposition region. However, we were able to show that heat transfer modeling is a viable method for determining a safe d_{f-s} distance in the HWCVD reactor.

Conflicts of Interest: The authors declare that they have no conflicts of interest to report regarding the present study.

References

1. Wiesmann, H., Ghosh, A. K., McMahon, T., Strongin, M. (1979). a-Si:H produced by high-temperature thermal decomposition of silane. *Journal of Applied Physics, 50(5),* 50–3752. DOI 10.1063/1.326284.
2. Atluri, S. N., Han, Z., Shen, S. (2003). Meshless Local Patrov-Galerkin (MLPG) approaches for weaklysingular traction & displacement boundary integral equations. *Computer Modeling in Engineering & Sciences, 4(5),* 507–517.
3. Wiesmann, H. (1980). US Patent 4 237 150, December 2.
4. Sali, J. V., Patil, S., Jadkar, S., Takwale, M. (2001). Hot-wire CVD growth simulation for thickness uniformity. *Thin Solid Films, 395(1–2),* 66–70. DOI 10.1016/S0040-6090(01)01209-3.

5. Lee, J., Kang, K., Kim, S., Yoon, K., Song, J. et al. (2001). The influence of filament temperature on crystallographic properties of poly-Si films prepared by the hot-wire CVD method. *Thin Solid Films, 395(1–2),* 188–193. DOI 10.1016/S0040-6090(01)01251-2.

6. Schüttauf, J. W. A., der Werf, C. H. M., van Sark, W. G. J. H. M., Rath, J. K., Schropp, R. E. I. et al. (2011). Comparison of surface passivation of crystalline silicon by a-Si:H with and without atomic hydrogen treatment using hot-wire chemical vapor deposition. *Thin Solid Films, 519(14),* 4476–4478. DOI 10.1016/j.tsf.2011.01.319.

7. Umemoto, H., Ohara, K., Morita, D., Nozaki, Y., Masuda, A. et al. (2002). Direct detection of H atoms in the catalytic chemical vapor deposition of the SiH_4/H_2 system. *Journal of Applied Physics, 91(3),* 1650–1656. DOI 10.1063/1.1428800.

8. Venkatesh, B. V. (2016). Tutorial of convective heat transfer in a vertical slot. *Proceedings of CFD with OpenSource Software*. Edited by Nilsson H. *http://www.tfd.chalmers.se/~hani/kurser/OS_CFD_2016*.

9. Rahman, U. A., Mustapha, F. (2015). Validations of OpenFOAM® steady state compressible solver rhoSimpleFoam. *International Conference on Mechanical and Industrial Engineering, Feb. 8–9, 2015. Kuala Lumpur, Malaysia*.

10. Greenshields, C. (2016). Computational fluid dynamics. *https://cfd.direct/openfoam/computational-fluid-dynamics/*.

11. Nozaki, F. (2016). buoyantPimpleFoam and buoyantSimpleFoam in OpenFOAM. *http://caefn.com/openfoam/solvers-buoyantpimplefoam*.

12. Matsumura, H., Masuda, A., Izumi, A. (1999). CAT-CVD process and its application to preparation of Si-based thin films. *MRS Proceedings, 557,* 1277. DOI 10.1557/PROC-557-67.

13. Matsumura, H. (1998). Formation of silicon-based thin films prepared by catalytic chemical vapor deposition (Cat-CVD) method. *Japanese Journal of Applied Physics, 37(6R),* 3175–3187. DOI 10.1143/JJAP.37.3175.

14. Karasawa, M., Masuda, A., Ishibashi, K., Matsumura, H. (2001). Development of Cat-CVD apparatus a method to control wafer temperatures under thermal influence of heated catalyzer. *Thin Solid Films, 395(1–2),* 71–74. DOI 10.1016/S0040-6090(01)01210-X.